

## Absence of Fermi-Level Pinning at Cleaved Nonpolar InN Surfaces

Chung-Lin Wu (吳忠霖),<sup>1,\*</sup> Hong-Mao Lee (李弘賢),<sup>1</sup> Cheng-Tai Kuo (郭承泰),<sup>1</sup>  
Chia-Hao Chen (陳家浩),<sup>2</sup> and Shangjr Gwo (果尚志)<sup>1,+</sup>

<sup>1</sup>Department of Physics, National Tsing-Hua University, Hsinchu 30013, Taiwan

<sup>2</sup>National Synchrotron Radiation Research Center (NSRRC), Hsinchu 30076, Taiwan

(Received 20 March 2008; published 4 September 2008)

Prior experimental work had found that the Fermi level at InN growth surfaces is pinned well above the conduction band edge, leading to strong surface band bending and electron accumulation. Using cross-sectional scanning photoelectron microscopy and spectroscopy, we show definitive evidence of unpinned Fermi level for *in situ* cleaved *a*-plane InN surfaces. To confirm the presence or absence of band bending, the surface Fermi level relative to the valence band edge was precisely measured by using both the Fermi edge of Au reference sample and the core level of ultrathin Au overlayer. It is confirmed that flat surface bands only occur at cleaved nonpolar surfaces, consistent with the recent theoretical predictions.

DOI: 10.1103/PhysRevLett.101.106803

PACS numbers: 73.20.At, 71.20.Nr, 79.60.Bm

Indium nitride (InN), because of its narrow direct band gap [1,2] and superior electron transport properties, has recently emerged as a technologically important semiconductor for use in near-infrared optoelectronics, high-efficiency solar cells, and high-speed electronics. The current obstacle for extensive fundamental studies and widespread applications of InN is mostly related to its unique surface electronic properties, resulting from the exceptionally large electron affinity. In particular, it has been found that the growth surfaces of InN exhibit a striking phenomenon that an intrinsic electron accumulation layer can form in the near-surface region of *n*-type InN. This phenomenon has been experimentally confirmed by a variety of different techniques [3,4]. A large downward band bending was observed with the surface Fermi-level ( $E_F$ ) pinned well above the conduction band minimum (CBM,  $E_C$ ), which is even more extreme than that at the indium arsenide (InAs) surfaces (the only other III-V compound semiconductor which exhibits this phenomenon) [5,6]. This pinning position induces a two-dimensional electron gas at the surface. Recently, quantum states of electrons in the InN surface accumulation layer have been directly observed by high-resolution angle-resolved photoemission spectroscopy [7]. Moreover, the electron accumulation phenomenon was also found to be present at the surfaces of *p*-type InN [8], resulting in the formation of a surface inversion layer which masks the bulk *p*-type conductivity and makes the realization of InN-based device applications extremely difficult. Therefore, at present, it is of utmost importance to resolve the difficulty related to the unique surface electronic properties of InN.

The origin of the electron accumulation at the InN surfaces has been explained by the unusual position of branch-point energy  $E_B$  (also called as charge neutrality level or Fermi-level stabilization energy) in InN [9,10], which has recently been determined to be about 1.83 eV above the valence-band maximum (VBM,  $E_V$ ) [11]. This implies that  $E_B$  is well above the CBM in InN since the

band gap energy ( $E_g$ ) of InN has been known to be about 0.65 eV. Until now, this phenomenon had been thought to be universal for all growth surfaces of InN films, independent of surface preparation method, growth polarity (N-polar, In-polar, or nonpolar), and crystal structure (wurtzite or metastable zinc-blende phase) [12].

Recently, based on their first-principles calculations, Segev and Van de Walle suggested that the microscopic origin of donor-type surface states is mostly associated with In-In bonding states on the InN surfaces with In adlayers. Furthermore, they have predicted that the phenomenon of surface electron accumulation will be absent on reconstructed nonpolar InN surfaces without In adlayers [13]. However, group-III metal adlayers, independent of the growth polarity, are favorable on the growth surfaces of III-nitrides, especially for the InN surfaces [14–16]. In this Letter, we report the first experimental evidence that *in situ* cleaved *a*-plane InN surfaces exhibit flat surface bands. By contrast, all the growth surfaces of InN ( $-c$ - and *a*-plane) studied by us and others exhibit a large downward surface band bending.

For this study, a wurtzite N-polar ( $-c$ -axis,  $[000\bar{1}]$ -oriented), undoped InN/GaN/AlN heterostructure, consisting of a 2.4- $\mu\text{m}$ -thick InN top layer, a 1.8- $\mu\text{m}$ -thick GaN intermediate layer, and a 1- $\mu\text{m}$ -thick AlN bottom layer, was grown by plasma-assisted molecular beam epitaxy (PA-MBE) on Si (111). The detailed growth process was described elsewhere [17]. The formation of relaxed InN, GaN, and AlN lattices in this heterostructure with the  $-c$ -axis perpendicular to the Si(111) plane was confirmed by synchrotron-radiation x-ray diffraction. All nitride epilayers were found to follow the following epitaxial relationship:  $\langle \bar{1} \bar{1} 20 \rangle_{\text{InN/GaN/AlN}} \parallel [\bar{1} 10]_{\text{Si}}$ . The unintentional *n*-type carrier concentration in the InN layer was determined by Hall measurement to be  $1.2 \times 10^{18} \text{ cm}^{-3}$  (it should be noted that the bulk carrier density might be lower due to surface electron accumulation). Using the nitride epilayer samples grown on Si substrates, *in situ* cleavage

becomes a viable approach to expose the clean, nonpolar  $\{\bar{1}\bar{1}20\}$  surface (i.e., the  $a$ -plane) under ultrahigh vacuum (UHV) conditions.

To investigate the cleaved surfaces which present a small cross section on the order of a few  $\mu\text{m}$ , a special experimental technique, cross-sectional scanning photoelectron microscopy and spectroscopy (SPEM/S) [18], was applied to achieve the required spatial resolution. The experiments were carried out at the 09A1 beam line of the National Synchrotron-Radiation Research Center (NSRRC), Hsinchu, Taiwan. Samples were cleaved under UHV conditions in the SPEM/S chamber, in order to reveal clean and well ordered cross-sectional surfaces. The SPEM/S system used here utilizes a combination of Fresnel zone plate and order sorting aperture to focus the monochromatic (380 eV) soft x ray (Fig. 1). The beam size at the focal plane is about 100–200 nm. The imaged samples were raster scanned relative to the focused x-ray spot. The emitted photoelectrons are synchronized collected by a multiple-channel hemispherical electron energy analyzer. By setting the electron collecting energy window of the analyzer to a characteristic core-level emission while raster-scanning the sample, a two-dimensional distribution of that particular element can be mapped.

The surface cleavage quality was confirmed by scanning electron microscopy (SEM). Figure 2(a) shows the SPEM image of a cleaved  $a$ -plane InN cross-sectional surface, corresponding to the spatial distribution of In  $4d$  core-level emission. Figure 2(b) presents the micro photoelectron spectroscopy ( $\mu$ -PES) spectrum taken on the InN region.

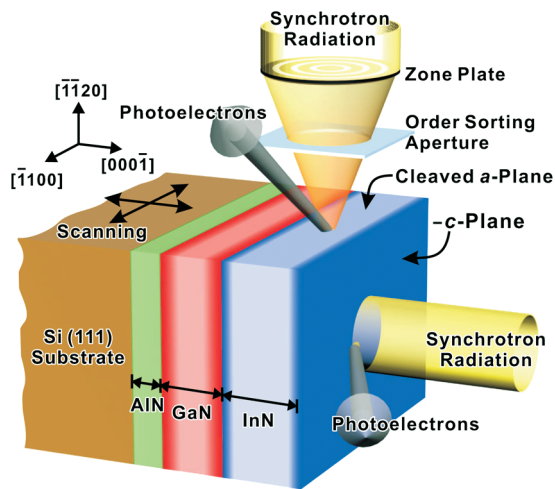


FIG. 1 (color). Sample probing geometry used in cross-sectional SPEM/S for studying wurtzite III-nitride heterostructures grown on Si(111) along the polar  $-c$ -axis. Conventional measurement geometry is also shown for comparison. The  $a$ -plane cross section is produced by *in situ* cleavage, and then placed under the focused synchrotron-radiation spot for chemical mapping and  $\mu$ -PES measurements. In this work, both methods were applied for *in situ* cleaved and as-grown surfaces, respectively.

The measured binding energy difference between the In  $4d$  core-level and the InN VBM is 16.84 eV ( $E_{\text{In } 4d} - E_V$ ). It should be noted that this value is a material constant, independent of crystal polarity and band bending effects, and it is in good agreement with that reported earlier for InN [19,20].

In order to examine the presence or absence of surface band bending using the PES technique, it is necessary to measure the VBM to surface Fermi-level energy separation (i.e.,  $E_V - E_F$ ). A downward band bending can be inferred if the surface  $E_F$  lies much higher in energy above the CBM than the bulk  $E_F$ . In contrast, under flat surface band conditions, the measured surface  $E_V - E_F$  should be very close to the bulk value ( $\sim E_g$  for the present  $n$ -type InN case). In Fig. 2(b), the binding energy scale is relative to the Fermi-level, which was calibrated with the Fermi edge of a clean Au reference sample placed on the same holder and was checked immediately before or after the  $\mu$ -PES measurements of freshly cleaved InN surfaces, as shown in the inset of Fig. 2(b). The measured values of  $E_V - E_F$  at several cleaved  $a$ -plane surfaces of InN all fall into the range of  $0.50 \pm 0.10$  eV. It should be noted that this value is much lower than the reported  $E_V - E_F$  values (1.4–1.8 eV) in the literature [11] and is very close to the expected bulk Fermi-level position ( $\sim E_g$ ), indicating the absence of band bending for the *in situ* cleaved  $a$ -plane InN surface.

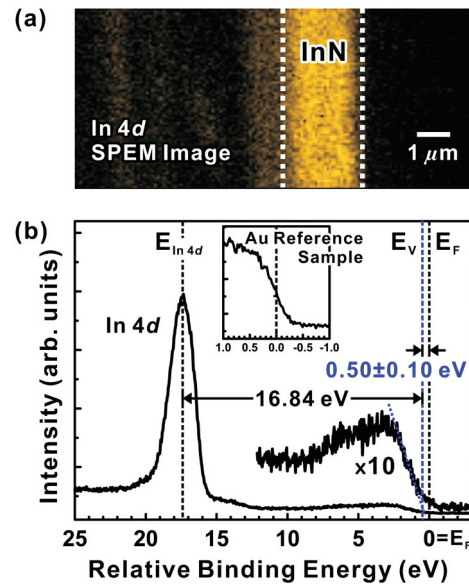


FIG. 2 (color). (a) SPEM image of the  $a$ -plane cleavage surface of an InN epitaxial layer. The In  $4d$  chemical mapping acquired by SPEM shows a good agreement with the growth structure. (b)  $\mu$ -PES spectrum taken on the region of InN layer. By linearly extrapolating the leading edge of the valence-band spectrum to the base line, the VBM position can be precisely located. The binding energy scale is relative to the Fermi-level, which was calibrated with the Fermi edge of a clean Au reference sample, as shown in the inset.

In addition, *in situ* deposition of an ultrathin metal layer on a clean InN surface can also be used to determine the surface  $E_F$  position [20]. However, the unusually large affinity in InN implies the possibility of induced downward band bending resulting from metal-adlayer donor-type states. In such a case, the Fermi-level might be moved closer to  $E_B$  ( $\sim 1.8$  eV above the VBM) than that before metal deposition. Here, we choose Au as the contact metal because the fact that it has the highest electronegativity and a large work function among metals (in the Pauling's electronegativity scale, Au: 2.54, In: 1.78, Cs: 0.79). For the case of cleaved InN surfaces with an *in situ* deposited Au overlayer, we used the Au core level (Au  $4f_{7/2}$ ) for precise measurement of the  $E_V - E_F$  value at the cleaved  $a$ -plane InN surface. In PES, the Au  $4f_{7/2}$  energy level ( $74.0 \pm 0.1$  eV relative to the Au Fermi edge) is common to be used as an "internal" reference because of its small intrinsic linewidth. The second material parameter which we can utilize is the  $E_{\text{In } 4d} - E_V$  constant [shown in

Fig. 2(b)]. By using this material parameter, after locating the position of surface  $E_F$ , the energy separation of  $E_V - E_F$  can be derived from the binding energy of In  $4d$  core level relative to  $E_F$ .

In our study, an ultrathin ( $\sim 6$  ML) Au layer was deposited by a carefully calibrated electron-beam evaporator onto the cleaved  $a$ -plane surfaces. The Au film morphology was checked by SEM to be very smooth. Figure 3(a) shows a  $\mu$ -PES spectrum obtained after Au deposition, in which all of the PES peaks associated with the Au  $4f$  and In  $4d$  core levels, as well as the valence bands (Au and InN) and the Au Fermi edge [see the inset of Fig. 3(a)] are visible. By aligning the In  $4d$  core-level of the  $\mu$ -PES spectrum before and after Au deposition, the value of  $E_V - E_F$  can be inferred to be  $0.50 \pm 0.10$  eV ( $= 17.34 - 16.84$  eV), as shown in the inset of Fig. 3(a). Compared to the as-cleaved case, the measured  $E_V - E_F$  value on the cleaved InN surface covered with an ultrathin Au layer is in the same range within our energy resolution ( $\pm 0.1$  eV), indicating that the Au overlayer does not induce significant surface band bending.

In Fig. 3(b), we illustrate the key difference between the cleaved and growth surfaces of InN using PES data obtained on *the same sample* ( $-c$ - vs  $a$ -face, see Fig. 1). For this measurement, the growth surface was partially coated with a Au overlayer through a shadow mask. By using a broad synchrotron-radiation beam, the Fermi edge technique can be applied to determine the  $E_V - E_F$  value. The obtained value of  $1.54 \pm 0.10$  eV is in good agreement with previous reports and indicates a large downward band

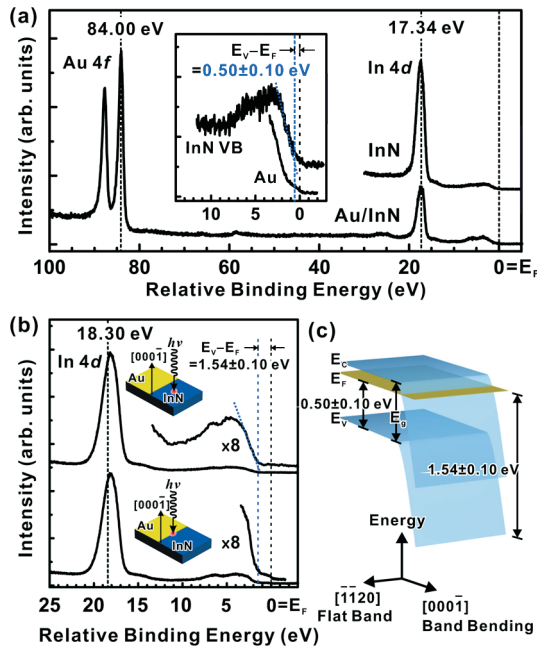


FIG. 3 (color). Photoelectron spectra of cleaved and grown surfaces of InN for determination of the VBM to surface Fermi-level energy separations ( $E_V - E_F$ ). (a)  $\mu$ -PES spectra measured from the cleaved  $a$ -plane InN surface before and after *in situ* deposition of an ultrathin Au overlayer. Using this technique, the Au  $4f$  and In  $4d$  core levels and the Au Fermi edge can all be resolved in the same spectrum for precise measurement of  $E_V - E_F$ . The binding energy scale is relative to the Au Fermi edge. (b) PES spectra measured with a broad synchrotron-radiation beam on the grown  $-c$ -plane InN surface. This surface was partially coated with a Au overlayer through a shadow mask, and the insets show the measurement positions. (c) Two-dimensional energy-band diagram of cleaved and growth surfaces of InN based on the measured values of  $E_V - E_F$  in (a) and (b).

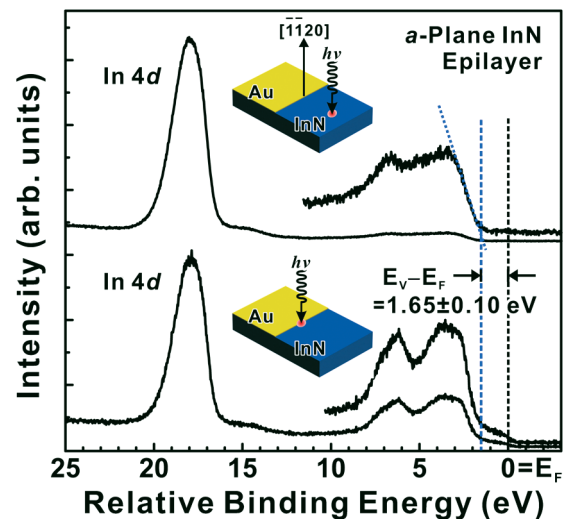


FIG. 4 (color). Photoelectron spectra of an epitaxial  $a$ -plane InN film grown on  $r$ -plane sapphire. This film was partially covered with a Au overlayer. The PES spectra were measured on the Au-free region (upper) and on the interface region (lower), respectively. The spectra are aligned to the In  $4d$  core-level, revealing the energy separation of 1.65 eV between the VBM (determined from the Au-free region) and the surface Fermi-level (determined from the Au/InN interface region).



bending [12]. It should be noted that the binding energy of In  $4d$  relative to the surface Fermi-level is 18.30 eV as determined by using the bulk-derived In  $4d$  component (the fitting procedure is described in Ref. [19] for InN growth surfaces). This binding energy is about 1 eV larger than that on the cross-sectional  $a$ -plane surface, which is another strong indication of large difference in surface band bending. Besides, the measured  $E_{\text{In}4d} - E_V$  value on the  $-c$ -plane growth surface is 16.76 eV, consistent with the value obtained on the cross-sectional surface of the same sample. Figure 3(c) displays the two-dimensional energy-band diagram based on the measured  $E_V - E_F$  values and the known band gap energy of InN. It can be clearly seen that the absence of surface band bending only occurs at the cleaved  $a$ -plane surface of InN.

For comparison, Fig. 4 shows the PES spectra obtained from the *growth surface* of an  $a$ -plane InN film partially coated with a Au overlayer. This film was grown on an  $r$ -plane  $\{1\bar{1}0\}$  sapphire substrate by PA-MBE with an  $n$ -type carrier concentration of  $1.3 \times 10^{19} \text{ cm}^{-3}$ . From previous theoretical and experimental studies, it has been suggested that the growth surfaces of InN are covered by In adlayers, independent of the film polarity [15,16]. Since the microscopic origin of surface donor states has been suggested to be In-In bonding states due to the In adlayers, it is important to compare between cleaved and grown  $a$ -plane surfaces of InN. Indeed, for the as-grown surface, we have confirmed a  $E_V - E_F$  value of  $1.65 \pm 0.10$  eV, indicative of the existence of large downward surface band bending.

It is interesting to compare the present findings with the known results for the nonpolar InAs surfaces. In particular, it has been known that, on the freshly cleaved InAs(110) surface, the surface accumulation layer is initially absent and is formed after gas and metal adsorption [21–23]. Depending on the chemical species of adsorbates, the surface Fermi-level was found to shift 0.1–0.6 eV above the CBM. Aristov *et al.* also reported that the metal-induced band bending has the trend of inverse proportionality with the electronegativities of metal adlayers [22]. This correlation could be explained by the charge transfer between the metal adlayer and the underlying semiconductor, resulting from the difference in their electronegativities [24]. We suggest that a similar mechanism might also exist for the present metals-on-InN case.

In summary, we provide here the definite evidence for the existence of unpinned nonpolar InN surfaces. Experimental data unambiguously show the absence of band bending for the *in situ* cleaved  $a$ -plane InN surface.

In contrast, all the growth surfaces of InN (polar or non-polar) with In adlayers exhibit a large downward surface band bending. Furthermore, our results indicate that the *in situ* deposited gold overlayer could serve as a good metallic contact for the unpinned InN surface without inducing significant surface band bending.

This work was supported by grants from the National Science Council, Taiwan. The authors would like to thank Joel W. Ager III of LBNL for helpful discussions.

---

\*Present address: Department of Physics, National Cheng Kung University, Tainan 701, Taiwan

+Corresponding author: gwo@phys.nthu.edu.tw

- [1] V. Yu. Davydov *et al.*, Phys. Status Solidi B **229**, R1 (2002).
- [2] J. Wu *et al.*, Appl. Phys. Lett. **80**, 3967 (2002).
- [3] H. Lu *et al.*, Appl. Phys. Lett. **82**, 1736 (2003).
- [4] I. Mahboob *et al.*, Phys. Rev. Lett. **92**, 036804 (2004).
- [5] M. Noguchi, K. Hirakawa, and T. Ikoma, Phys. Rev. Lett. **66**, 2243 (1991).
- [6] L. Ö. Olsson *et al.*, Phys. Rev. Lett. **76**, 3626 (1996).
- [7] L. Colakerol *et al.*, Phys. Rev. Lett. **97**, 237601 (2006).
- [8] R. E. Jones *et al.*, Phys. Rev. Lett. **96**, 125505 (2006).
- [9] I. Mahboob *et al.*, Phys. Rev. B **69**, 201307(R) (2004).
- [10] S. X. Li *et al.*, Phys. Rev. B **71**, 161201(R) (2005).
- [11] P. D. C. King *et al.*, Phys. Rev. B **77**, 045316 (2008).
- [12] P. D. C. King *et al.*, Appl. Phys. Lett. **91**, 092101 (2007).
- [13] D. Segev and C. G. Van de Walle, Europhys. Lett. **76**, 305 (2006); C. G. Van de Walle and D. Segev, J. Appl. Phys. **101**, 081704 (2007); D. Segev and C. G. Van de Walle, J. Cryst. Growth **300**, 199 (2007).
- [14] A. R. Smith *et al.*, Phys. Rev. Lett. **79**, 3934 (1997); J. E. Northrup *et al.*, Phys. Rev. B **61**, 9932 (2000).
- [15] D. Segev and C. G. Van de Walle, Surf. Sci. **601**, L15 (2007).
- [16] T. D. Veal *et al.*, Phys. Rev. B **76**, 075313 (2007).
- [17] S. Gwo *et al.*, Appl. Phys. Lett. **84**, 3765 (2004); C.-L. Wu *et al.*, Appl. Phys. Lett. **87**, 241916 (2005).
- [18] C.-L. Wu *et al.*, Appl. Phys. Lett. **92**, 162106 (2008).
- [19] C.-L. Wu *et al.*, Appl. Phys. Lett. **91**, 042112 (2007).
- [20] K. A. Rickert *et al.*, Appl. Phys. Lett. **82**, 3254 (2003).
- [21] Y. Chen, J. C. Hermanson, and G. J. Lapeyre, Phys. Rev. B **39**, 12682 (1989).
- [22] V. Yu. Aristov, Phys. Scr. **T39**, 333 (1991); V. Yu. Aristov *et al.*, Phys. Rev. B **47**, 2138 (1993); V. Yu. Aristov *et al.*, Europhys. Lett. **26**, 359 (1994).
- [23] M. Morgenstern *et al.*, Phys. Rev. B **61**, 13805 (2000); M. Getzlaff *et al.*, Phys. Rev. B **63**, 205305 (2001).
- [24] W. Mönch, *Electronic Properties of Semiconductor Interfaces* (Springer, Berlin, 2004), Chap. 5.